Special Issue on Chemistry

Microwave Assisted Green Synthesis of Copper Ferrite Spinel Nanoparticles using *Moringa oleifera* Leaf Extract

B. Kavitha, B. Muthu and A. Manikandan

Issue Editor
Dr. A. Manikandan

Research Journal of Agricultural Sciences
An International Journal

P- ISSN: 0976-1675
E- ISSN: 2249-4538

Volume: 13
Issue: Special

Res. Jr. of Agril. Sci. (2022) 13(S): 092–095

CARAS

Res. Jr. of Agril. Sci. (2022) 13(Special): 092–095

www.rjas.org

ISSN: 0976-1675 (P)
ISSN: 2249-4538 (E)

Full Length Research Article

Microwave Assisted Green Synthesis of Copper Ferrite Spinel Nanoparticles using *Moringa oleifera* Leaf Extract

B. Kavitha[1], B. Muthu[2] and A. Manikandan*[3]

Received: 08 Dec 2021 | Revised accepted: 15 Feb 2022 | Published online: 25 Feb 2022

A B S T R A C T

The present study focused on the preparation of spinel copper ferrite ($CuFe_2O_4$) nanoparticles with the metal nitrates of copper and iron by adopting microwave assisted green synthesis using *Moringa oleifera* leaf extract. The characterization of synthesized $CuFe_2O_4$ NPs was carried out by Powder XRD, FT-IR, SEM and VSM analyses. The $CuFe_2O_4$ NPs were then studied for their photocatalytic activity to degrade the organic dye Malachite green (MG). Spinel $CuFe_2O_4$ NPs was found to be the best catalyst for the photodegradation of MG dye. The PCD results revealed that the photodegradation of MG achieved at 92.5 % degradation was recorded.

Key words: *Moringa oleifera* leaf extract, Microwave assisted, $CuFe_2O_4$ NPs, Green synthesis photodegradation, Malachite green

A number of treatment technologies have evolved to degradae the pollution arising from organic pollutants [1-2]. These include the processes involving photocatalytic degradation (PCD) and photo-Fenton processes etc. such as Advanced Oxidation Processes (AOPs). However, PCD and AOPs were found to be associated with sludge formation in bulk materials and requirement of high operating costs [3]. Recently, the use of photocatalysts have increased high consideration for the removal of organic pollutants by using nanocatalysts as they involve lower costs and show little or no toxicity [4-5]. The physical and chemical stability of photocatalyst and their strong potential to completely mineralize the organic pollutants make them favorable for use [6-7].

The photocatalytic degradation of dyes work by the photosystem through UV or visible region or the both. During the reaction, photoexcited electrons get shifted from VB to CB, thereby generating a pair of electron/hole (e-/h+), which oxidizes or reduces the organic pollutants adsorbed onto the catalyst surface [8-10]. Semiconductor metal oxides exhibit their photocatalytic activity either by the creation of OH radicals or the O^{2-} radicals as a result of O_2 reduction. Both the anions and radicals (OH and O^{2-} radicals) have the potential to interact with the organic pollutants and convert them into slighter harmful by-products [11-15].

* **A. Manikandan**
manikandan.research@bharathuniv.ac.in

[1-3] Department of Chemistry, Bharath Institute of Higher Education and Research (BIHER), Chennai - 600 073, Tamil Nadu, India

The physical and chemical characteristics of metal oxides such as their surface morphology, crystal shape, crystallite size and precursors compositionsetc. Therefore, various methods have been approved to regulate the surface morphology, particle size and structure of the prepared materials [16-18]. Among them, spinel structure of copper ferrite ($CuFe_2O_4$) nanoparticles have attracted importance, due to their applications in catalysis due to their smaller size, higher surface to volume ratio as well as the magnetic interactions amongst particles. Most of the applications of $CuFe_2O_4$ NPs involved the treatment of bio medical applications. However, during the last few decades, $CuFe_2O_4$ NPs involved for the organic pollutants and dyes from the water bodies [19-22].

$CuFe_2O_4$ NPs belongs to the spinel minerals that have the formula AB_2O_4. The preparation conditions such as precursors, temperatures etc. decide the morphology of the $CuFe_2O_4$ NPs that govern the properties of the magnetic structure. In this regard, microwave assisted green synthesis using *Moringa oleifera* leaf extract offers better homogeneity ascompared to other techniques. $CuFe_2O_4$ ferrites as the potential photo catalysts for the photo-degradation of organic dye due to their cheaper costs and lower toxicity.

MATERIALS AND METHODS

Iron (III) nitrate, copper (II) nitrate (Sigma-Aldrich, 99%), used microwave assisted using *Moringa oleifera* leaf extract green synthesis of $CuFe_2O_4$ NPs. Deionized water was utilized in all stages of the synthesis. Malachite (MG) was purchased for the photocatalytic degradation. The *Moringa oleifera* leaf extract were washed with deionized water. Plant moisture was removed at 50 °C. To each gram of watercress powder, 10 ml of deionized water was added and shaken at

50°C, overnight. Finally, the extract was separated with Whatman paper and centrifuged. Iron (III) nitrate, copper (II) nitrate solution was added to 50 ml of aqueous extract. The mixture was kept in a microwave oven. The final product were washed well with DI water and ethanol twice finally dried at 70°C and used for further characterizations.

Characterization techniques

The structural characterization of $CuFe_2O_4$ NPs were performed using Rigaku Ultima X-ray diffractometer equipped with Cu-Kα radiation (λ =1.5418 Å). The surface functional groups were analyzed by Perkin Elmer FT-IR spectrometer. Morphological studies and energy dispersive X-ray analysis (EDX) of $CuFe_2O_4$ NPs have been performed with a Jeol JSM6360 high resolution scanning electron microscopy (HR-SEM). Magnetic measurements were carried out at room temperature using a PMC MicroMag 3900 model vibrating sample magnetometer equipped with 1 Tesla magnet.

RESULTS AND DISCUSSION

XRD analysis

The powder XRD pattern of $CuFe_2O_4$ NPs are depicted in the (Fig 1). The broader diffraction peaks were observed in XRD diffractograms that depicted the nano scale range of formed $CuFe_2O_4$ NPs. The XRD patterns recorded for the $CuFe_2O_4$ NPs powder showed a single-phase cubic spinel structure [23-25]. The lattice parameter calculated from XRD information is 8.397Å. The average crystallite size (15.85 nm) was calculated using sherrer formula and the calculated lattice constant are in good agreement with the earlier report.

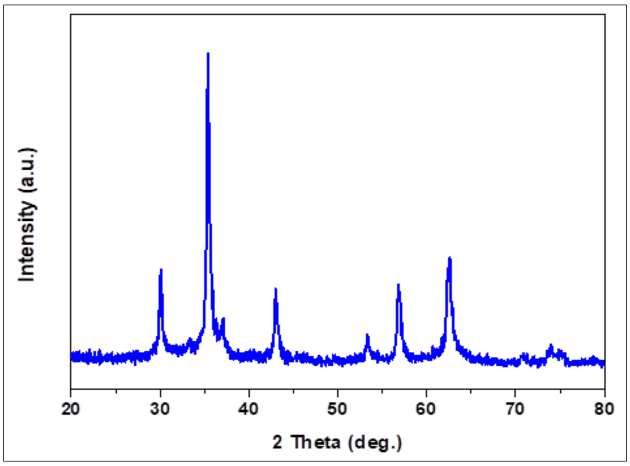

Fig 1 Powder XRD pattern of $CuFe_2O_4$ NPs

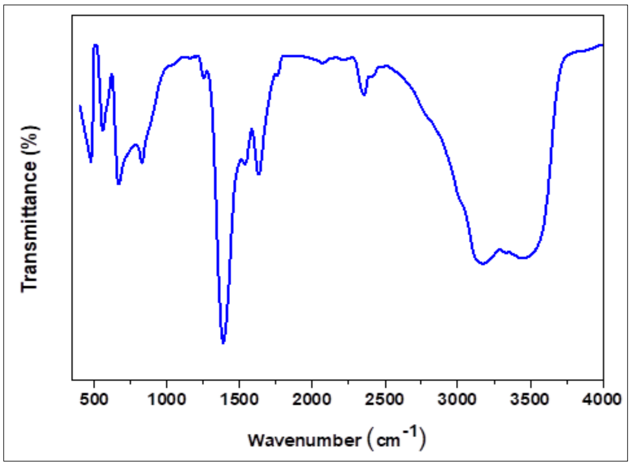

Fig 2 FT-IR spectra of $CuFe_2O_4$ NPs

FTIR technique

The FTIR spectrum of $CuFe_2O_4$ NPs are shown in (Fig 2). $CuFe_2O_4$ NPs astrong absorptions were observed at 400-600 cm-1 region, which is mainly due to the spinel structure. The band at 545 cm-1 was accredited to the octahedral (B-site) coordinated Cu atoms with O that corresponded to the spinel structure as reported in literature [26-28]. The vibration observed at 698 cm-1 was ascribed to the stretching vibrations for tetrahedral (A-site) coordinated Cu-O, whereas the bands at 693 and 421 cm-1 showed the formation of $CuFe_2O_4$ NPs. Two vibrations at 588 and 453 cm-1 indicated the vibration of Fe-O in tetrahedral (A-site) and octahedral (B-site) clusters respectively. The crystallinity of the prepared $CuFe_2O_4$ NPs was reflected by the sharpness of the peaks. The vibration at 1642 cm-1 depicted the water molecules adsorbed by the $CuFe_2O_4$ NPs on its surface [29-31].

SEM analysis

(Fig 3) depicts the surface morphology of $CuFe_2O_4$ NPs. All these particle sizes were dispersed uniformly. The sphere-shaped nanoparticles were defined with sharp boundaries. The particle sizes among the prepared $CuFe_2O_4$ NPs was similar to the XRD crystallite size. The size of particle was recorded in the range of 15-20 nm. In fact, $CuFe_2O_4$ NPs, the particles are magnetic in nature, which causes their agglomeration and hence a larger size. The agglomeration of particles took place to form the larger ones. Good contact was observed between particles that were with well-defined sharp grain boundaries.

VSM analysis

The magnetic measurements was analysed by VSM analysis and the results of $CuFe_2O_4$ NPs at room temperature (RT) and ±10 kOe applied field are shown in Figure 5. The amount of magnetic saturation (M_s) for the synthesized $CuFe_2O_4$ NPs was 39.62emu/g. The obtained result shows superparamagnetic properties [32-35]. Additionally, the amount of magnetic saturation of $CuFe_2O_4$ NPs depends on their size, crystallinity and structure [36,37]. The spinel structure and superparamagnetic behaviour of $CuFe_2O_4$ NPs were confirmed by XRD and VSM analyses.

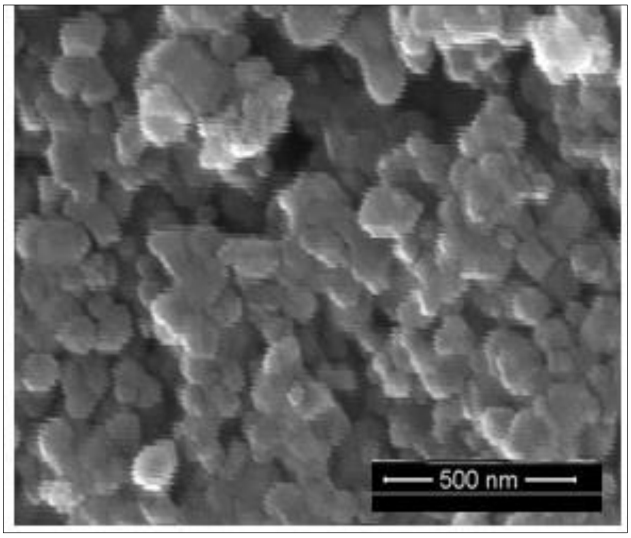

Fig 3 SEM image of $CuFe_2O_4$ NPs

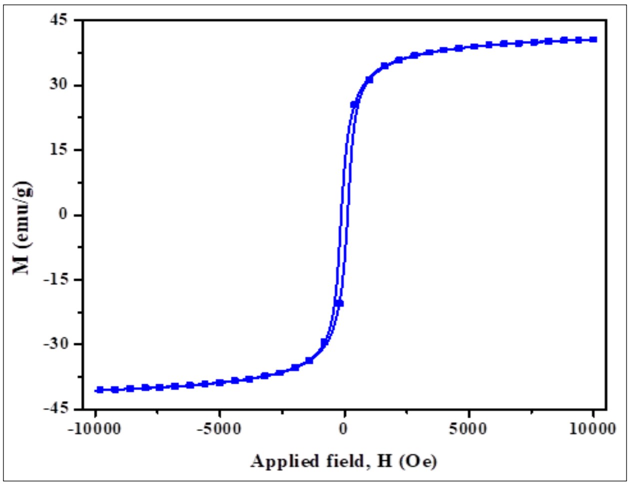

Fig 4 Magnetic properties of $CuFe_2O_4$ NPs

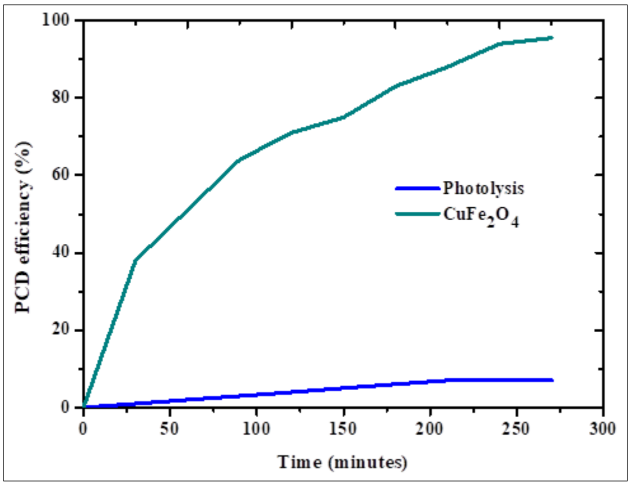

Fig 5 PCD efficiency of $CuFe_2O_4$ NPs

Photodegradation analysis

To select the best performance photocatalyst, MG dye degradation was determined in the presence of $CuFe_2O_4$ NPs separately under optimum conditions and the efficiency of dye degradation was recorded (Fig. 5). Dye degradation performance achieved at 92.5 % degradation in 180 minutes which was fairly in agreement with its crystallinity as revealed by SEM. In the dark environment, there is no availability of photons to energize the dye degradation process, while under the UV set-up, the production light and acceleration of electron-hole pair increases, which leads to increased hydroxyl ions and eventually speeding up the degradation process [35-37].

CONCLUSION

The present study focused on the preparation of spinel copper ferrite ($CuFe_2O_4$) nanoparticles with the metal nitrates of copper and iron by adopting microwave assisted green synthesis using *Moringa oleifera* leaf extract. The characterization of synthesized $CuFe_2O_4$ NPs was carried out by Powder XRD, FT-IR, SEM and VSM analyses. The $CuFe_2O_4$ NPs were then studied for their photocatalytic activity to degrade the organic dye Malachite green (MG). Spinel $CuFe_2O_4$ NPs was found to be the best catalyst for the photodegradation of MG dye. The PCD results revealed that the photodegradation of MG achieved at 92.5 % degradation was recorded.

Acknowledgment

The authors are thankful to Tamil Nadu State Council for Science and Technology (TNSCST), DOTE Campus, Chennai for the financial support (S&T Project: TNSCST/ STP-PRG/AR/2018-2019/9307).

LITERATURE CITED

1. A. Manikandan, R. Sridhar, S. A. Antony, S. Ramakrishna, A simple aloe vera plant-extracted microwave and conventional combustion synthesis: Morphological, optical and catalytic properties of magnetic $CoFe_2O_4$ nanostructures, J. Mol. Struct., 1076 (2014) 188-200.
2. N. Babitha, L. Srimathi Priya, S. Rosy Christy, A. Manikandan, A. Dinesh, M. Durka, and S. Arunadevi, Enhanced Antibacterial Activity and Photo-Catalytic Properties of ZnO Nanoparticles: Pedalium Murex Plant Extract-Assisted Synthesis, J. Nanoscie. Nanotech. 19 (2019) 2888–2894.
3. K. Chitra, A. Manikandan, S. Arul Antony, Effect of poloxamer on Zingiber officinale extracted green synthesis and antibacterial studies of silver nanoparticles, J. Nanoscie. Nanotech. 16 (2016) 758-764.
4. A. Manikandan, M. Durka, S. Arul Antony, Hibiscus rosa-sinensis leaf extracted green methods, magneto-optical and catalytic properties of spinel $CuFe_2O_4$ nano- and microstructures, J. Inorg. Organomet. Polym., 25 (2015) 1019–1031.
5. K. Chitra, K. Reena, A. Manikandan, S. Arul Antony, Antibacterial studies and effect of poloxamer on gold nanoparticles by Zingiber officinale extracted green synthesis, J. Nanoscie. Nanotech. 15 (2015) 4984-4991.
6. K. Chitra, A. Manikandan, S. Moortheswaran, K. Reena, S. Arul Antony, Zingiber officinale extracted green synthesis of copper nanoparticles: Structural, morphological and antibacterial studies, Adv. Sci. Eng. Med., 7 (2015) 710-716.
7. A. Manikandan, M. Durka, M. A. Selvi, S. Arul Antony, Sesamum indicum plant extracted microwave combustion synthesis and opto-magnetic properties of spinel $Mn_xCo_{1-x}Al_2O_4$ nano-catalysts, J. Nanoscie. Nanotech. 16 (2016) 448-456.
8. A. Manikandan, M. Durka, M. A. Selvi, S. Arul Antony, Aloe vera plant extracted green synthesis, structural and opto-magnetic characterizations of spinel $Co_xZn_{1-x}Al_2O_4$ nano-catalysts, J. Nanoscie. Nanotech. 16 (2016) 357-373.
9. P. Bhavani, A. Manikandan, P. Paulraj, A. Dinesh, M. Durka, and S. Arul Antony, Okra (Abelmoschus esculentus) Plant Extract-Assisted Combustion Synthesis and Characterization Studies of Spinel $ZnAl_2O_4$ Nano-Catalysts, J. Nanoscie. Nanotech. 18 (2018) 4072–4081.
10. D. Maruthamani, S. Vadivel, M. Kumaravel, B. Saravanakumar, B. Paul, S. Sankar Dhar, A. H. Yangjeh, A. Manikandan, G. Ramadoss, Facile synthesis of Bi_2O_3/reduced graphene oxide (RGO) nanocomposite for supercapacitor and visible light photocatalytic applications, J. Colloid Interf. Sci., 498 (2017) 449-459.
11. A. Shameem, P. Devendran, V. Siva, M. Raja, A. Manikandan, S. A. Bahadur, Preparation and characterization studies of nanostructured CdO thin films by SILAR method for photocatalytic applications, J. Inorg. Organomet. Polym., 27 (2017) 692–699.
12. A. Silambarasu, A. Manikandan, K. Balakrishnan, Room temperature superparamagnetism and enhanced photocatalytic activity of magnetically reusable spinel $ZnFe_2O_4$ nano-catalysts, J. Supercond. Nov. Magn., 30 (2017) 2631–2640.

13. R. Bomila, S. Srinivasan, S. Gunasekaran, A. Manikandan, Enhanced photocatalytic degradation of methylene blue dye, opto-magnetic and antibacterial behaviour of pure and La-doped ZnO nanoparticles, J. Supercond. Nov. Magn., 31 (2018) 855–864.
14. I. J. C. Lynda, M. Durka, A. Dinesh, A. Manikandan, S. K. Jaganathan, A. Baykal, S. Arul Antony, Enhanced Magneto-optical and Photocatalytic Properties of Ferromagnetic $Mg_{1-y}Ni_yFe_2O_4$ (0.0 ≤ y ≤ 1.0) Spinel Nano-ferrites, J. Supercond. Nov. Magn., 31 (2018) 3637–3647.
15. S. Velanganni, A. Manikandan, J. Joseph Prince, C. Neela Mohan, R. Thiruneelakandan, Nanostructured ZnO coated Bi_2S_3 thin films: Enhanced photocatalytic degradation of Methylene blue dye, Physica B, 545 (2018) 383-389.
16. J. A. H. Sheela, S. Lakshmanan, A. Manikandan, S. A. Antony, Structural, morphological and optical properties of ZnO, $ZnO:Ni^{2+}$ and $ZnO:Co^{2+}$ nanostructures by hydrothermal process and their photocatalytic activity, J. Inorg. Organomet. Polym. 28 (2018) 2388–2398.
17. R. A. Senthil, S. Osman, J. Pan, Y. Sun, T. R. Kumar, A. Manikandan, A facile hydrothermal synthesis of visible-light responsive $BiFeWO_6/MoS_2$ composite as superior photocatalyst for degradation of organic pollutants, Ceram. Int., 45 (2019) 18683-18690.
18. R. A. Senthil, S. Osman, J. Pan, A. Khan, V. Yang, T. R. Kumar, Y. Sun, A. Manikandan, One-pot preparation of AgBr/α-Ag_2WO_4 composites with superior photocatalytic activity under visible-light irradiation, Colloids and Surf. A: Physicochem. Eng. Aspects, 586 (2020) 124079.
19. S. Rathinavel, R. Deepika, D. Panda, A. Manikandan, Synthesis and characterization of $MgFe_2O_4$ and $MgFe_2O_4$/rGO nanocomposites for the photocatalytic degradation of methylene blue, Inorg. Nano-Metal Chem., 51, 2 (2021) 210-217.
20. A Muthukrishnaraj, SS Kalaivani, A Manikandan, Helen P Kavitha, R Srinivasan, N Balasubramanian, Sonochemical synthesis and visible light induced photocatalytic property of reduced graphene oxide@ ZnO hexagonal hollow rod nanocomposite, J. Alloys Compds., 83625 (2020) 155377.
21. T. L. Ajeesha, A. Ashwini, Mary George, A. Manikandan, J. Arul Mary, Y. Slimani, M. A. Almessiere, A. Baykal, Nickel substituted $MgFe_2O_4$ nanoparticles via co-precipitation method for photocatalytic applications, Physica B, 606 (2021) 412660.
22. R. Renuga, A. Manikandan, J. A. Mary, A. Muthukrishnaraj, A. Khan, S. Srinivasan, B. Abdullah M. Al Alwan and K. M. Khedher, Enhanced Magneto-Optical, Morphological, and Photocatalytic Properties of Nickel-Substituted SnO_2 Nanoparticles, J. Supercond. Nov. Magn., 34 (2021) 825–836.
23. M. George, T.L. Ajeesha, A. Manikandan, Ashwini Anantharaman, R.S. Jansi, E. Ranjith Kumar, Y. Slimani, M.A. Almessiere, A. Baykal, Evaluation of Cu-$MgFe_2O_4$ spinel nanoparticles for photocatalytic and antimicrobial activates, J. Phys. Chem. Solids, 153 (2021) 110010.
24. K. Geetha, R. Udhayakumar, A. Manikandan, Enhanced magnetic and photocatalytic characteristics of cerium substituted spinel $MgFe_2O_4$ ferrite nanoparticles, Physica B, 615 (2021) 413083.
25. C. Sambathkumar, V. Manirathinam, A. Manikandan, M. Krishna Kumar, S. Sudhakar, P. Devendran, Solvothermal synthesis of Bi_2S_3 nanoparticles for active photocatalytic and energy storage device applications, J. Mater. Sci. Mater. Elect., 32 (2021) 20827-20843.
26. SP Ratnayake, M Mantilaka, C Sandaruwan, D Dahanayake, E Murugan, Carbon quantum dots-decorated nano-zirconia: a highly efficient photocatalyst, Applied Catalysis A: General, 2019, 570, 23-30.
27. E Murugan, I Pakrudheen, Efficient amphiphilic poly (propylene imine) dendrimer encapsulated ruthenium nanoparticles for sensing and catalysis applications, Science of Advanced Materials, 2015, 7 (5), 891-901.
28. E Murugan, JN Jebaranjitham, A Usha Synthesis of polymer-supported dendritic palladium nanoparticle catalysts for Suzuki coupling reaction, Applied Nanoscience, 2012, 2 (3), 211-222
29. E Murugan, SS Kumar, KM Reshna, S Govindaraju, Highly sensitive, stable g-CN decorated with AgNPs for SERS sensing of toluidine blue and catalytic reduction of crystal violet, Journal of Materials Science 2019, 54 (7), 5294-5310
30. E Murugan, S Santhoshkumar, S Govindaraju, M Palanichamy, Silver nanoparticles decorated g-C3N4: An efficient SERS substrate for monitoring catalytic reduction and selective Hg2+ ions detection, Spectrochimica Acta Part A: Molecular and Biomolecular Spectroscopy, 2021, 246, 119036.
31. R. R. Mathiarasu, A. Manikandan, K. Panneerselvam, M. George, Y. Slimani, M. A. Almessiere, A. Baykal, A. M. Asiri, T. Kamal, A. Khan, Photocatalytic degradation of reactive anionic dyes RB5, RR198 and RY145 via Rare earth element (REE) Lanthanum substituted $CaTiO_3$ perovskite catalysts, Journal of Materials Research and Technology, 15 (2021) 5936-5947.
32. A. Alagarsamy, S. Chandrasekaran, A. Manikandan, Green synthesis and characterization studies of biogenic zirconium oxide (ZrO_2) nanoparticles for adsorptive removal of methylene blue dye, Journal of Molecular Structure, 1247 (2022) 131275.
33. V. S. P. Sakthi Sri, A. Manikandan, M. Mathankumar, R. Tamizhselvi, M. George, A. L. Bilgrami, S. A. Al-Zahrani, A. A. P. Khan, Anish Khan, A. M. Asiri, Unveiling the photosensitive, mechanical and magnetic properties of amorphous iron nanoparticles with its application towards decontamination of water and cancer treatment, Journal of Materials Research and Technology, 15 (2021) 99-118.
34. K. Geetha, R. Udhayakumar, A. Manikandan, Enhanced magnetic and photocatalytic characteristics of cerium substituted spinel $MgFe_2O_4$ ferrite nanoparticles, Physica B: Physics of Condensed Matter, 615 (2021) 413083.
35. A. Muthukrishnaraj, S. A. Al-Zahrani, A. Al Otaibi, S. S. Kalaivani, A. Manikandan, N. Balasubramanian, A. L. Bilgrami, M. A. R. Ahamed, A. Khan, A. M. Asiri, N. Balasubramanian, Enhanced Photocatalytic Activity of Cu_2O Cabbage/RGO Nanocomposites under Visible Light Irradiation, Polymers, 13 (2021) 1712.
36. P. Annie Vinosha, A. Manikandan, A. Christy Preetha, A. Dinesh, Y. Slimani, M.A. Almessiere, A. Baykal, Belina Xavier, G. Francisco Nirmala, Review on recent advances of synthesis, magnetic properties and water treatment applications of cobalt ferrite nanoparticles and nanocomposites, Journal of Superconductivity and Novel Magnetism, 34 (2021) 995–1018.
37. P. A. Vinosha, A. Manikandan, A. S. J. Ceicilia, A. Dinesh G. F. Nirmala, A. Christy Preetha, Y. Slimani, M.A. Almessiere, A. Baykal, B. Xavier, Review on recent advances of zinc substituted cobalt ferrite nanoparticles: Synthesis characterization and diverse applications. *Ceramics International* 47(2021) 10512-10535.